J|A|C|S
ARTICLES
Published on Web 12/31/2003

Characterization of μs−ms Dynamics of Proteins Using a Combined Analysis of ^{15}N NMR Relaxation and Chemical Shift: Conformational Exchange in Plastocyanin Induced by Histidine Protonations

Mathias A. S. Hass,[†] Marianne H. Thuesen,[‡] Hans E. M. Christensen,[‡] and Jens J. Led*,[†]

Contribution from the Department of Chemistry, University of Copenhagen, The H. C. Ørsted Institute, Universitetsparken 5, DK-2100 Copenhagen Ø, Denmark, and Department of Chemistry, The Technical University of Denmark, Building 207, DK-2800 Lyngby, Denmark

Received June 19, 2003; E-mail: led@kiku.dk

Abstract: An approach is presented that allows a detailed, quantitative characterization of conformational exchange processes in proteins on the μs−ms time scale. The approach relies on a combined analysis of NMR relaxation rates and chemical shift changes and requires that the chemical shift of the exchanging species can be determined independently of the relaxation rates. The applicability of the approach is demonstrated by a detailed analysis of the conformational exchange processes previously observed in the reduced form of the blue copper protein, plastocyanin from the cyanobacteria *Anabaena variabilis* (*A.v.* PCu) (Ma, L.; Hass, M. A. S.; Vierick, N.; Kristensen, S. M.; Ulstrup, J.; Led, J. J. *Biochemistry* **2003**, *42*, 320−330). The R_1 and R_2 relaxation rates of the backbone ^{15}N nuclei were measured at a series of pH and temperatures on an ^{15}N labeled sample of *A.v.* PCu, and the ^{15}N chemical shifts were obtained from a series of HSQC spectra recorded in the pH range from 4 to 8. From the R_1 and R_2 relaxation rates, the contribution, R_{ex}, to the transverse relaxation caused by the exchanges between the different allo-states of the protein were determined. Specifically, it is demonstrated that accurate R_{ex} terms can be obtained from the R_1 and R_2 rates alone in the case of relatively rigid proteins with a small rotational anisotropy. The R_{ex} terms belonging to the same exchange process were identified on the basis of their pH dependences. Subsequently the identifications were confirmed quantitatively by the correlation between the R_{ex} terms and the corresponding chemical shift differences of the exchanging species. By this approach, the R_{ex} terms of ^{15}N nuclei belonging to contiguous regions in the protein could be assigned to the same exchange process. Furthermore, the analysis of the exchange terms shows that the observed μs−ms dynamics in *A.v.* PCu are caused primarily by the protonation/deprotonation of two histidine residues, His92 and His61, His92 being ligated to the Cu(I) ion. Also the exchange rate of the protonation/deprotonation process of His92 and its pH and temperature dependences were determined, revealing a reaction pathway that is more complex than a simple specific-acid/base catalysis. Finally, the approach allows a differentiation between two-site and multiple-site exchange processes, thus revealing that the protonation/deprotonation of His61 is at least a three-site exchange process. Overall, the approach makes it feasible to obtain exchange rates that are sufficiently accurate and versatile for studies of the kinetics and the mechanisms of local protein dynamics on the sub-millisecond time scale.

Introduction

Protein function is intimately linked to local conformational changes in the protein molecules.[1] Moreover, numerous biological processes take place on the μs−ms time scale.[2−4] Insight into the dynamics on this time scale is, therefore, essential in order to understand the biological function of proteins. However, the detection of structural fluctuations on the μs−ms time scale is difficult, let alone a determination of the specific nature of the conformational changes and the kinetic and thermodynamic parameters that characterize the associated exchange processes.

NMR spectroscopy provides a powerful tool for studying such processes at equilibrium.[5−7] This is due to the fact that the relaxation rate, R_2, of the transverse nuclear magnetization is highly sensitive to conformational fluctuations on the μs−ms

[†] University of Copenhagen.
[‡] The Technical University of Denmark.

(1) Fersht, A. *Structure and Mechanism in Protein Science*; W. H. Freeman and Company: New York, 1998.
(2) Feher, V. A.; Cavanagh, J. *Nature* **1999**, *400*, 289−293.
(3) Volkman, B. F.; Lipson, D.; Wemmer, D. E.; Kern, D. *Science* **2001**, *291*, 2429−2433.
(4) Eisenmesser, E. Z.; Bosco, D. A.; Akke, M.; Kern, D. *Science* **2002**, *295*, 1520−1523.
(5) Palmer, A. G. *Curr. Opin. Struct. Biol.* **1997**, *7*, 732−737.
(6) Palmer, A. G.; Kroenke, C. D.; Loria, J. P. *Methods Enzymol.* **2001**, *339*, 204−238.
(7) Akke, M. *Curr. Opin. Struct. Biol.* **2002**, *12*, 642−647.

time scale. In recent years, the determination of the protein backbone dynamics from R_1 and R_2 relaxation rates of the backbone ^{15}N nuclei and the corresponding $\{^1H\}-^{15}N$ nuclear Overhauser effect (NOE) has become a standard procedure.[5,8,9] Usually a Lipari−Szabo model-free analysis[10,11] is applied to retrieve information about fast ps−ns fluctuations of the backbone. In addition, an exchange contribution, R_{ex}, to the R_2 rates, caused by μs−ms fluctuations, can also be determined. Qualitatively, the presence of an R_{ex} term indicates that the observed nucleus experiences a chemical shift fluctuation on the μs−ms time scale. However, the magnitude of the exchange terms depends on several normally unknown parameters. Thus, for a simple two-site exchange system,

$$A \rightleftarrows B \tag{1}$$

the exchange term as obtained from standard R_2 experiments[9] is given by[12]

$$R_{ex} = \Delta\delta^2\gamma^2B_0^2p_ap_b\frac{1}{k_{ex}}\left(1 - \frac{2}{\tau_{cp}k_{ex}}\tanh\left(\frac{\tau_{cp}k_{ex}}{2}\right)\right) \tag{2}$$

if the so-called fast exchange condition applies (see below). Here, k_{ex} is the rate constant of the exchange process, $\Delta\delta$ is the chemical shift difference between the two conformations, A and B, while p_a and p_b are the populations of A and B, respectively. Furthermore, B_0 is the magnetic field strength, γ is the gyromagnetic ratio, and τ_{cp} is the interpulse delay of the CPMG pulse-train applied in the R_2 experiment. Therefore, even though the exchange terms contain vital information about the exchange processes, it is not possible to extract this information from the R_1 and R_2 relaxation rates and $\{^1H\}-^{15}N$ NOEs of the backbone ^{15}N nuclei, unless independent information about $\Delta\delta$, p_a, and p_b can be obtained. In addition, three- or multisite exchange processes may be involved, just as more than one exchange process may contribute to an observed exchange term, or different exchange processes may affect structurally related nuclei. Consequently, the possibility of interpreting the R_{ex} data without additional information is rather limited.

To deconvolute the dynamic information of the R_{ex} data, several experimental techniques are available.[6] Thus, the Carr−Purcell−Meiboom−Gill (CPMG)[13,14] and the $R_{1\rho}$ relaxation dispersion techniques[15,16] as well as the field dependency of R_2 have been applied[17,18] to characterize the μs−ms dynamics in proteins. Depending on the time scale of the exchange process, the exchange rate, the equilibrium constant, and the chemical shift difference may be obtained from these experiments.[6]

An alternative approach is to determine the chemical shift differences and the equilibrium constant independently of the relaxation measurements. This is possible if the conformational exchange process is affected significantly by changes in the sample conditions, such as the temperature or the pH of the sample, or the concentration of a ligand that binds to the protein. By simultaneously monitoring the changes in both the relaxation rate and the chemical shift of the observed nuclei, it is, in principle, possible to characterize the exchange processes in detail. This approach is analogous to the classical methods based on chemical shift and line shape analyses that have been applied for decades to study chemical exchange processes by one-dimensional NMR spectroscopy.[19−21] However, because of extensive signal overlap, these are of limited use for large molecules. Yet, the principles can be transferred to large-dispersion, two-dimensional heteronuclear NMR,[22] where, furthermore, the R_2 rates can be obtained more accurately from HSQC based R_2 experiments than from line width measurements. This approach was previously used in studies of the dynamics of the Ca^{2+}-binding protein calmodulin[23,24] and in a study of the protein dynamics during catalytic action of the cis/trans isomerase, cyclophilin A.[4]

Here we investigate the general applicability of such an approach by measuring the ^{15}N relaxation rates and the ^{15}N chemical shifts of a protein at a series of different pH values and different temperatures. The protein in question is the reduced, diamagnetic form of the 105-amino acid (10.9 kDa) blue copper protein, plastocyanin from the cyanobacteria *Anabaena variabilis*[25] (*A.v.* PCu), while the processes being investigated are the μs−ms exchange processes previously observed in this protein. Thus, a recent study[26] of the backbone dynamics of reduced *A.v.* PCu showed that several regions of this electron-transferring protein are affected by μs−ms dynamics, including the copper site and the so-called "eastern face" of the molecule. Each of these regions contains a pH-titratable histidine side chain, viz. His92 at the copper site and His61 on the "eastern face". The observed dynamics might therefore be coupled to the exchange between the protonated and the deprotonated states of these two histidine residues. Moreover, protonation of His92 has a dramatic impact on the biological activity of reduced PCu. In the deprotonated state, the imidazole group of His92 is ligated to the Cu(I) ion and the protein is biologically active. Upon protonation, the imidazole−Cu(I) bond breaks, which leads to a rearrangement of both the copper site geometry and the His92 side chain.[27] As a consequence, the redox potential increases while PCu loses its biological activity.[25] His61, being located about 9 Å from the copper ion, is not part of the redox center. However, for other blue copper proteins, the protonation of similar remote histidines is known to affect the redox activity.[28−32] Therefore, histidine protonation

(8) Kay, L. E.; Torchia, D.; Bax, A. *Biochemistry* **1989**, *28*, 8972−8979.
(9) Farrow, N. A.; Muhandiram, R.; Singer, A. U.; Pascal, S. M.; Kay, C. M.; Gish, G.; Shoelson, S. E.; Pawson, T.; Forman-Kay, J. D.; Kay, L. E. *Biochemistry* **1994**, *33*, 5984−6003.
(10) Lipari, G.; Szabo, A. *J. Am. Chem. Soc.* **1982**, *104*, 4546−4559.
(11) Lipari, G.; Szabo, A. *J. Am. Chem. Soc.* **1982**, *104*, 4559−4570.
(12) Luz, Z.; Meiboom, S. *J. Chem. Phys.* **1963**, *39*, 366−370.
(13) Tollinger, M.; Skrynnikov, N. R.; Mulder, F. A. A.; Forman-Kay, J. D.; Kay, L. E. *J. Am. Chem. Soc.* **2001**, *123*, 11341−11352.
(14) Mulder, F. A. A.; Mittermaier, A.; Hon, B.; Dahlquist, F. W.; Kay, L. E. *Nat. Struct. Biol.* **2001**, *8*, 932−935.
(15) Akke, M.; Palmer, A. G. *J. Am. Chem. Soc.* **1996**, *118*, 911−912.
(16) Vugmeyster, L.; Kroenke, C. D.; Picart, F.; Palmer, A. G.; Raleigh, D. P. *J. Am. Chem. Soc.* **2000**, *122*, 5387−5388.
(17) Millet, O.; Loria, J. P.; Kroenke, C. D.; Pons, M.; Palmer, A. G. *J. Am. Chem. Soc.* **2000**, *122*, 2867−2877.
(18) Korzhnev, D. M.; Karlsson, B. G.; Orekhov, V. Y.; Billeter, M. *Protein Sci.* **2003**, *12*, 56−65.
(19) Sudmeier, J. L.; Evelhoch, J. L.; Jonsson, N. B.-H. *J. Magn. Reson.* **1980**, *40*, 377−390.
(20) Kaplan, J. I.; Fraenkel, G. *NMR of Chemical Exchanging Systems*; Academic Press: New York, 1980.
(21) Rao, B. D. *Methods Enzymol.* **1989**, *176*, 279−311.
(22) Günther, U.; Mittag, T.; Schaffhausen, B. *Biochemistry* **2002**, *41*, 11658−11669.
(23) Evenäs, J.; Forsén, S.; Malmendal, A.; Akke, M. *J. Mol. Biol.* **1999**, *289*, 603−617.
(24) Malmendal, A.; Evenäs, J.; Forsén, S.; Akke, M. *J. Mol. Biol.* **1999**, *293*, 883−899.
(25) Hope, A. B. *Biochim. Biophys. Acta* **2000**, *1456*, 5−26.
(26) Ma, L.; Hass, M. A. S.; Vierick, N.; Kristensen, S. M.; Ulstrup, J.; Led, J. J. *Biochemistry* **2003**, *42*, 320−330.
(27) Guss, J. M.; Harrowell, P. R.; Murata, M.; Norris, V. A.; Freeman, H. C. *J. Mol. Biol.* **1986**, *192*, 361−387.
(28) Sigfridsson, K.; Hansson, O.; Karlsson, B. G.; Baltzer, L.; Nordling, M.; Lundberg, L. G. *Biochim. Biophys. Acta* **1995**, *1228*, 28−36.

may provide an important regulatory mechanism in plastocyanin as well as in other blue copper proteins. An investigation of the correlation between the μs−ms dynamics and the protonation of histidines in plastocyanin may provide new information on the function of blue copper proteins.

Results and Discussion

pH Dependence of the Backbone ^{15}N Chemical Shifts. The approach presented here requires an independent determination of the chemical shift difference between the exchanging species. To investigate whether the exchange between the protonated and the deprotonated form of *A.v.* PCu gives rise to the exchange terms observed previously,[26] the pH variation of the chemical shifts of all the 95 observable backbone ^{15}N amide nuclei was analyzed. Thus, the difference in ^{15}N chemical shift between the protonated and deprotonated states of PCu, both with respect to His92 and His61, was determined for each residue whenever possible.

Primarily, the analysis included a determination of the pK_a values of His92 and His61. Initially the ^{15}N chemical shift titration data were fitted to

$$\delta_{obs} = \delta_d + \frac{\Delta\delta}{1 + 10^{[pH-pK_a]}} \qquad (3)$$

Here, δ_{obs} are the observed chemical shifts and $\Delta\delta = \delta_p - \delta_d$, where δ_p and δ_d is the chemical shift of the protonated and the deprotonated state, respectively. For most of the ^{15}N nuclei with significantly pH dependent chemical shifts, the pH variations correspond to a pK_a value in the ranges 4.9−5.3 or 6.9−7.3 in agreement with the pK_a values of His92 and His61. However, the chemical shifts of several residues are affected by both of these titrations. In these cases, the pH variations were fitted to

$$\delta_{obs} = \delta_d + \frac{\Delta\delta_1}{1 + 10^{[pH-pK_{a1}]}} + \frac{\Delta\delta_2}{1 + 10^{[pH-pK_{a2}]}} \qquad (4)$$

In eq 4, it is assumed that the two protonation processes are independent of each other. Here, $\Delta\delta_1$ and $\Delta\delta_2$ are the chemical shift changes associated with pK_{a1} and pK_{a2}, respectively, and δ_d is the chemical shift of the deprotonated state with respect to both processes. In the cases where $\Delta\delta_1$ and $\Delta\delta_2$ have opposite signs, all five parameters in eq 4 were fitted, that is, δ_d, $\Delta\delta_1$, $\Delta\delta_2$, pK_{a1}, and pK_{a2}, while in the cases where $\Delta\delta_1$ and $\Delta\delta_2$ have the same sign, one of the two pK_a values was fixed at 5.1 or 7.2. In a few cases with very small $\Delta\delta$ values, both pK_a values were fixed at 5.1 and 7.2, respectively.

Using eqs 3 and 4, it was found that a total of 53 backbone ^{15}N nuclei are affected by a titration with a pK_a value in the range from 4.9 to 5.3 and that 42 of these nuclei have $|\Delta\delta| \geq 0.1$ ppm. Similarly, a total of 51 backbone ^{15}N nuclei are affected by a titration with a pK_a value in the range from 6.9 to 7.3, 26 of which have $|\Delta\delta| \geq 0.1$ ppm. Examples of the obtained chemical shift titration curves are shown in Figure 1, while the overall result of the chemical shift analysis is given in Figure 2a and 2b. A complete list of the fitted parameters is given in the Supporting Information.[33]

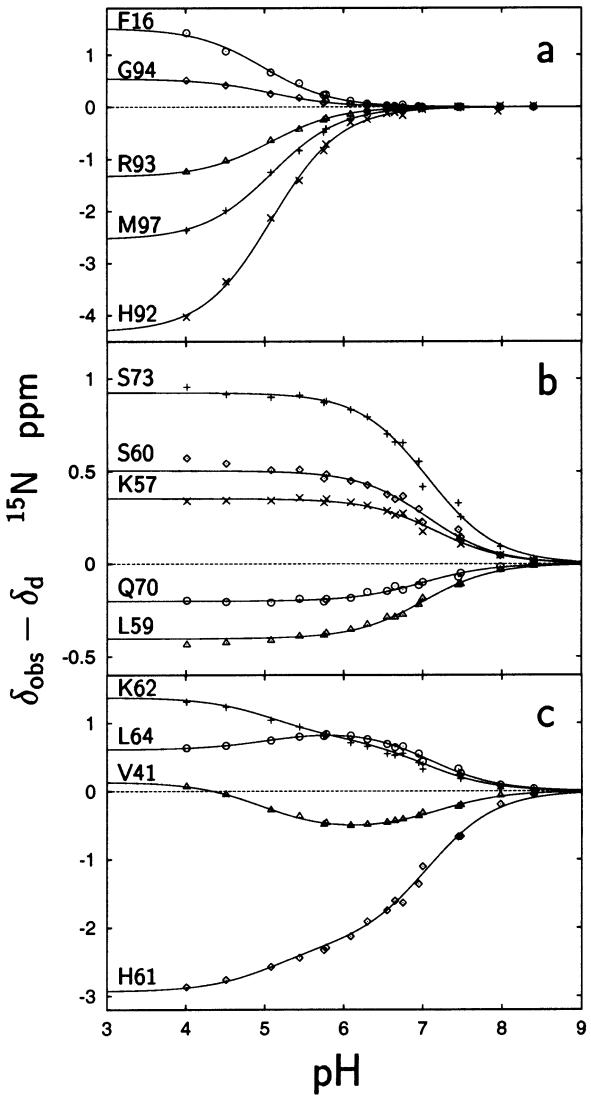

Figure 1. Backbone ^{15}N chemical shift titration curves for selected residues: (a) residues that titrate with a pK_a value of 5.1 ± 0.1 corresponding to the protonation of His92; (b) residues that titrate with a pK_a value of 7.1 ± 0.1 corresponding to protonation of His61; (c) residues that are affected by the titration of both His92 and His61. The curves in part a and b represent a least-squares fit of eq 3, while the curves in part c represent a least-squares fit of eq 4.

For 21 of the backbone ^{15}N nuclei, pK_a values below 4.9 were obtained. In *A.v.* PCu, these pK_a values can only be associated with carboxylate groups, although they are less precise, since only two spectra below pH 5 were recorded. Overall it is found that only in a few cases the chemical shift perturbation from the titration of the carboxylate groups interferes with that of the histidines. Thus, most likely the pK_a value of Glu30 is almost identical to that of His92 (see below). It is, therefore, not possible to distinguish between the effect from the titration of Glu30 and His92 only on the basis of the chemical shift titration curves. This distinction, however, can be made on the basis of the correlation between the titration shifts, $|\Delta\delta|$, and the exchange terms, R_{ex}, as shown below. The average pK_a for His92

(29) Kalverda, A. P.; Ubbink, M.; Gilardi, G.; Wijmenga, S. S.; Crawford, A.; Jeuken, L. J. C.; Canters, G. W. *Biochemistry* **1999**, *38*, 12690−12697.
(30) Canters, G. W.; Kolczak, U.; Armstrong, F.; Jeuken, L. J. C.; Camba, R.; Sola, M. *Faraday Discuss.* **2000**, *116*, 205−220.
(31) Dennison, C.; Lawler, A. T. *Biochemistry* **2001**, *40*, 3158−3166.
(32) Sato, K.; Dennison, C. *Biochemistry* **2002**, *41*, 120−130.

(33) The ^{15}N chemical shifts and the ^{15}N relaxation data of *A.v.* PCu are deposited in the BioMagResBank (http://www.bmrb.wisc.edu) under accession number 5858.

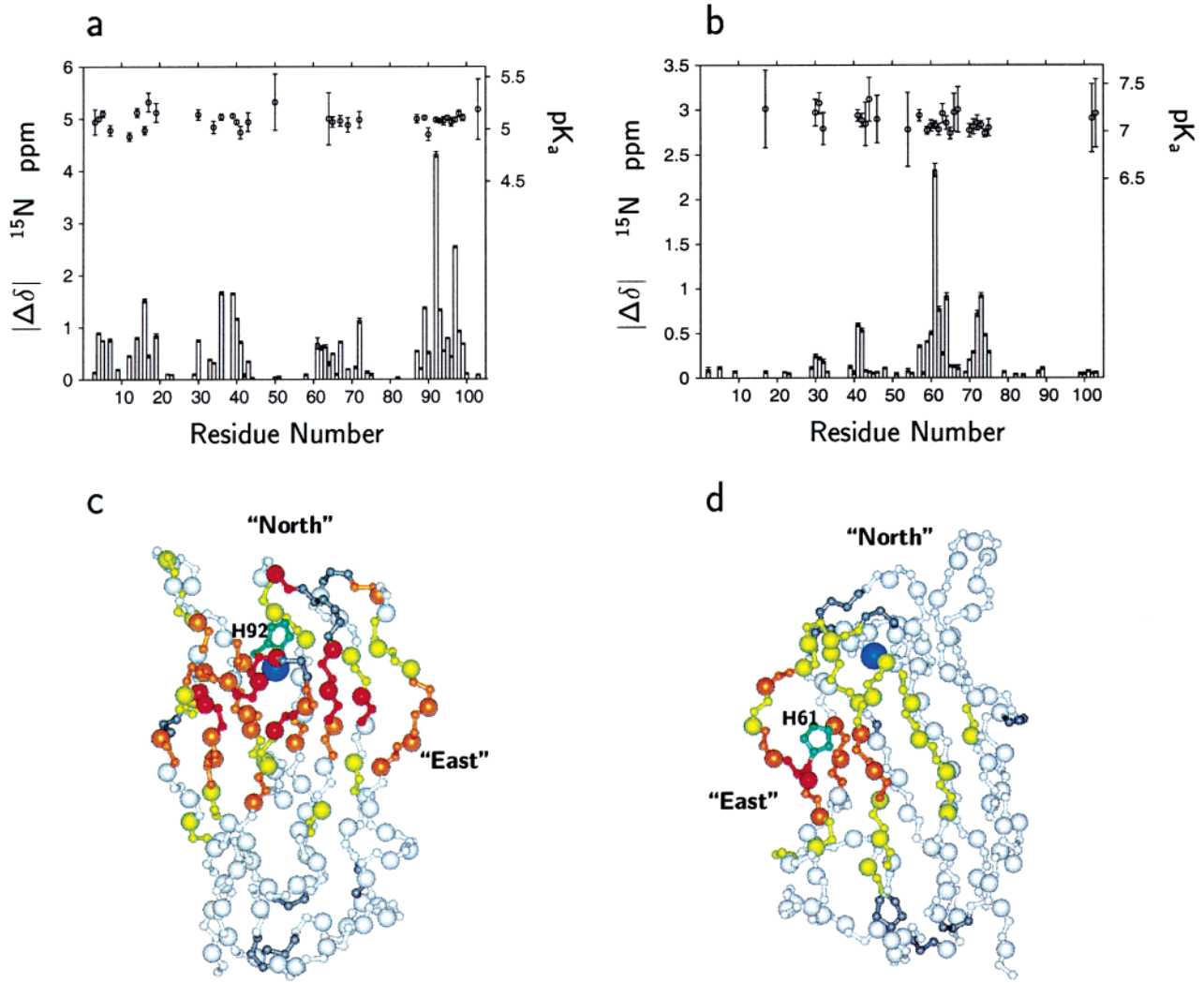

Figure 2. Chemical shifts changes, $|\Delta\delta|$, of the backbone ^{15}N nuclei in *A.v.* PCu upon protonation of His92 (a and c) and His61 (b and d). In parts a and b, the $|\Delta\delta|$ values are given as bars, while the pK_a values obtained from the individual residue are shown as data points (top of parts a and b). In parts c and d, the size of the $|\Delta\delta|$ shifts of the individual ^{15}N nuclei are indicated by color codes in the structure of *A.v.* PCu (PDB entry 1FA4):[35,36] red, $|\Delta\delta| > 1.0$ ppm; orange, $|\Delta\delta| = 0.5-1.0$ ppm; yellow, $|\Delta\delta| = 0.1-0.5$ ppm; light gray, $|\Delta\delta| < 0.1$ ppm. The nitrogen atoms are marked as spheres. The copper ion is shown as a dark blue sphere, and prolines are colored dark gray. The relevant histidine side chain is colored green. In part d, the structure is rotated approximately 180° around a vertical axis relative to part c.

obtained from the titration curves of 33 nuclei was 5.09 ± 0.01, in close agreement with the value of 5.1 found previously.[34] For His61, the average pK_a determined from 28 nuclei was 7.06 ± 0.02, a value slightly lower than the value of 7.3 previously reported.[34]

Relation Between the Structure and the ^{15}N Chemical Shift Changes. The residues with chemical shift changes corresponding to a pK_a of 5.1 ± 0.2 cluster isotropically around the copper site of PCu (see Figure 2c). The various effects that contribute to the ^{15}N chemical shift dispersion are not sufficiently well understood to allow a conversion of the observed chemical shift changes into structural information.[37] However, two main contributions to the change in chemical shift may be considered: (1) the increased positive charge at the metal site upon protonation and (2) a spatial rearrangement of the His92 side chain and the copper site geometry. The latter rearrangement may be mediated throughout the backbone, thereby affecting the structure relatively far away from the His92 imidazole group and the copper coordination sphere. Indeed, the protonation of His92 does change the geometry of the copper site.[25,27,32] However, a comparison of the X-ray structures of PCu from *Populus nigra* at different pH values indicate only subtle rearrangements upon protonation.[27] These rearrangements are mainly located at the copper coordination sphere and consist of a 180° rotation of the His92 imidazole group and a ring flip of Pro38 from the C^2 exo to the C^2 endo conformation. The backbone structure remains almost unchanged in the crystal structures.[27] Hence, it is an open question to what extent the observed changes in chemical shift are caused by a structural rearrangement or by the change in the electric field caused by the increased positive charge of the copper site.

The residues with chemical shift changes corresponding to a pK_a of 7.1 ± 0.2 cluster around the imidazole group of His61,

(34) Kojiro, C. L.; Markley, J. L. *FEBS Lett.* **1983**, *162*, 52−56.
(35) Badsberg, U.; Jørgensen, A. M. M.; Sørensen, G. O.; Ulstrup, J.; Led, J. J. *J. Am. Chem. Soc.* **1996**, *35*, 7021−7031.
(36) Ma, L.; Jørgensen, M. A.-M.; Sørensen, G. O.; Ulstrup, J.; Led, J. J. *J. Am. Chem. Soc.* **2000**, *122*, 9473−9485. 35. Wishhart, D. S.; Case, D. A. *Methods Enzymol.* **2001**, *338*, 3−34.
(37) Wishhart, D. S.; Case, D. A. *Methods Enzymol.* **2001**, *338*, 3−34.

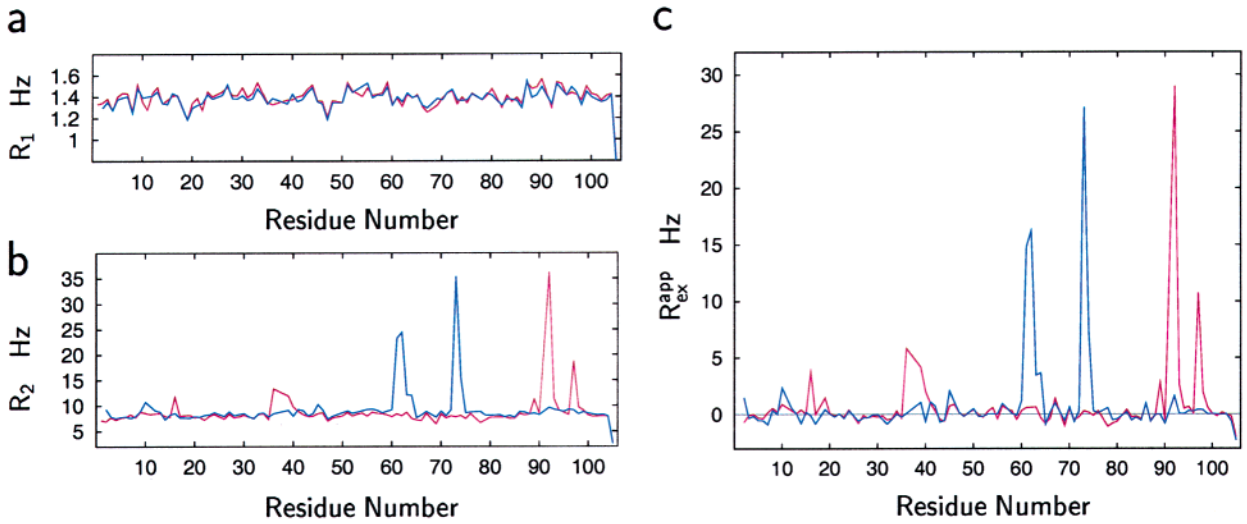

Figure 3. (a) R_1 relaxation rates and (b) R_2 relaxation rates of the backbone ^{15}N nuclei in *A.v.* PCu versus the amino acid sequence at pH 4.60 (red) and at pH 7.46 (blue). (c) The approximate exchange terms, R_{ex}^{app} (see text), at both pH values were calculated from the R_1 and the R_2 rates in parts a and b using eq 7.

as shown in Figure 2d. In general, smaller chemical shift changes are observed as compared to those arising from the protonation of His92.

pH and Temperature Dependence of the Backbone ^{15}N Relaxation: Indication of Specific Exchange Processes. An almost complete set of R_1 and R_2 relaxation rates for the 95 assigned backbone nitrogens (the 9 prolines and the two first N-terminal residues not included) was obtained at 11 different pH values.[33] Also the R_1 and R_2 rates at pH 5.8 were measured at four different temperatures. A list of the relaxation parameters obtained at two different pH values is given in the Supporting Information. For a few residues, reliable relaxation rates could not be obtained at some of the pH values because of a large signal overlap or because fast exchange of the protons with the solvent made the signals unobservable in the HSQC spectrum at high pH.

As shown in Figure 3a, the measured R_1 rates are independent of pH within the experimental uncertainties. This indicates that the backbone flexibility on the ps-ns time scale is largely unaffected by pH in the investigated pH range. In contrast, dramatic pH-dependent variations of the R_2 rates are observed in two regions (Figure 3b), indicating large changes in the μs−ms dynamics of *A.v.* PCu in the applied pH range from pH 4.2 to pH 8.5. Thus, residues close to the copper site, including His92, have large R_2 rates at a pH around 5, where the interconversion between the protonated and deprotonated forms of His92 takes place. Similarly, residues close to the imidazole group of His61 have large R_2 rates at a pH around 7, where the interconversion between the protonated and deprotonated forms of His61 is effective. Immediately, these results suggest that the observed μs−ms dynamics in *A.v.* PCu is closely related to the protonation of the two surface-exposed histidines, His92 and His61.

To investigate the nature and the characteristics of the exchange processes, the contributions, R_{ex} (eq 2), to the R_2 relaxation rates of the backbone ^{15}N nuclei were examined together with their pH and temperature dependencies. The R_{ex} terms were obtained using the average R_2/R_1 ratios, as detailed below, while the reliability of these ratios and their pH and temperature dependencies were evaluated by the corresponding dependencies of the rotational correlation time, τ_{rot}, derived from the ratios.[8]

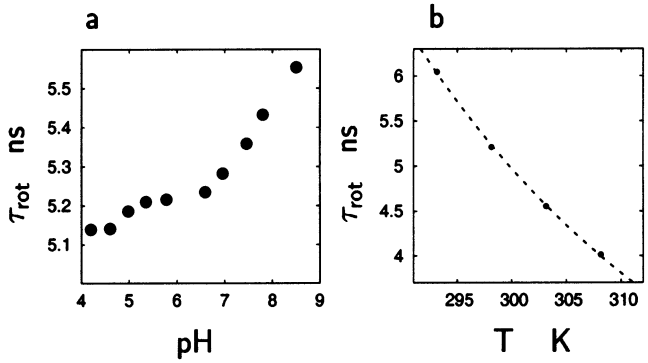

Figure 4. Rotational correlation time, τ_{rot}, versus (a) pH at 398 K and versus (b) temperature at pH 5.8. The dashed line represents the least-squares fit to the Stokes−Einstein relation. The size of the symbols reflect the uncertainty of τ_{rot}.

pH and Temperature Dependence of the Rotational Diffusion. The isotropic rotational correlation time was calculated from the average R_2/R_1 ratio (see Experimental Section). As shown in Figure 4, τ_{rot} increases by 8% over the investigated pH range (4.2−8.5). Although this increase is small, the trend is clear and systematic indicating an increased self-association at higher pH. This could reflect a decreasing intermolecular repulsion, caused by the decrease of the overall net charge of *A.v.* PCu when approaching the isoelectric pH of 8.4.[38]

The rotational correlation time also depends on the temperature, mainly through the temperature dependence of the water viscosity. As shown in Figure 4b, τ_{rot} decreases by about 30% when the temperature is raised from 20 to 35 °C. The temperature dependence was analyzed using the Stokes−Einstein relation, $\tau_{rot} = V_p\eta/k_BT$, where V_p is the protein volume, k_B is the Boltzmann constant, and η is the viscosity. The latter depends exponential on the inverse temperature, that is, $\eta \propto$

(38) Davis, D. J.; Krogman, D. W.; Pieto, A. S. *Plant Physiol.* **1980**, *65*, 697−702.

$\exp(E_a/k_BT)$. An analysis of the data in Figure 4b using this model resulted in an activation energy of the rotational diffusion of $E_a = 18.1 \pm 0.3$ kJ/mol. This value is in agreement with the activation energy of 16.7 ± 0.2 kJ/mol of the viscosity of pure H_2O in the same temperature range.[39] Consequently, the pH and temperature dependency of τ_{rot} confirm the reliability of the average R_2/R_1 ratios.

Determination of the Exchange Terms. An exchange term, R_{ex}, for each of the observed backbone ^{15}N nuclei was estimated from the measured R_2 and R_1 rates. The R_2 rates consist of three contributions, one from dipolar relaxation, R_2^{dip}, one from chemical shift anisotropy (CSA) relaxation, R_2^{CSA}, and one from chemical exchange, R_{ex}. Thus,

$$R_2 = R_2^0 + R_{ex} \tag{5}$$

where $R_2^0 = R_2^{dip} + R_2^{CSA}$ is the transverse relaxation rate in the absence of chemical exchange. The R_2^0 term depends on fast internal motion and rotational diffusion. The R_2^0 rate is determined most accurately from the R_1 rates, the NOEs, and the longitudinal and transverse CSA-dipol cross-correlation rates.[40] However, the R_2^0 rate can be estimated from the corresponding R_1 rate and the average R_2/R_1 ratio alone, that is

$$R_2^0 \approx R_1\left\langle\frac{R_2}{R_1}\right\rangle \tag{6}$$

Therefore, the following approximate exchange term, R_{ex}^{app}, can be obtained using eq 5:

$$R_{ex}^{app} = R_2 - R_1\left\langle\frac{R_2}{R_1}\right\rangle \tag{7}$$

Equation 6 assumes that the rotational diffusion is isotropic. This holds to a good approximation for the PCu molecule, where the rotational anisotropy was found to be insignificant ($D_\parallel/D_\perp = 1.15$).[26] Furthermore, eq 6 assumes that local ps−ns dynamics is very fast, the internal correlation time, τ_i, being <100 ps. In general, this is a good assumption for rigid molecules such as plastocyanins.[26,41] Possible errors caused by this approximation will, if they are significant, result in an underestimation of the exchange term[42] and may lead to nonphysical, negative R_{ex}^{app} values. As shown in Figure 3c, a few residues have large negative R_{ex}^{app} values. Thus, at pH 5.8 and 25 °C, a total of 25 residues have R_{ex}^{app} values smaller than −0.2 Hz, while 12 of these are less than −0.5 Hz and only two of these are smaller than −1.0 Hz. Therefore, the error introduced by eq 7 is unlikely to exceed 1 Hz and will only affect the relatively small exchange terms significantly. Moreover, such errors can be effectively reduced by a small correction as shown below.

pH Dependence of the Exchange Terms: Identification of Exchange Terms Belonging to the Same Exchange Process. Most of the obtained R_{ex} terms in *A.v.* PCu depend strongly on pH. This dependence may be explained by the protonation/deprotonation processes of His92 and His61, corresponding to a simple two-site exchange:

$$D + H^+ \rightleftarrows PH^+ \tag{8}$$

Here the rate constants, k_{ex}, of these processes are defined as $k_{ex} = \tau_d^{-1} + \tau_p^{-1}$, where τ_d and τ_p are the lifetimes of the states D and PH^+, respectively. If the exchange process is in the fast exchange regime, i.e., $k_{ex} > |\gamma B_0 \Delta\delta|$, or if[17] $|\gamma B_0 \Delta\delta| \lesssim 1.5/\tau_{cp}$ (here corresponding to $|\Delta\delta| \lesssim 3$ ppm), the R_{ex} is proportional to $\Delta\delta^2$, that is

$$R_{ex} = a(\Delta\delta)^2 \tag{9}$$

where

$$a = \gamma^2 B_0^2 p_d p_p \frac{1}{k_{ex}}\left(1 - \frac{2}{\tau_{cp}k_{ex}}\tanh\left(\frac{\tau_{cp}k_{ex}}{2}\right)\right) \tag{10}$$

according to eq 2. Here p_d and p_p are the populations of the deprotonated and protonated state, respectively. The factor a must be identical for all ^{15}N nuclei affected by the same two-site exchange process. According to eq 10, the factor a depends on the exchange rate and the equilibrium population of the exchanging species, p_d and p_p. Provided that the exchange is well-described by eq 8, the product $p_d p_p$ is given by

$$p_d p_p = (2 + 10^{[pH - pK_a]} + 10^{[pK_a - pH]})^{-1} \tag{11}$$

with a maximum value of 0.25 at pH = pK_a. Accordingly, a and thereby R_{ex} reach a maximum at this pH value as shown in Figure 5a. This is strictly correct only if k_{ex} is independent of pH, which is normally not the case for protonation processes. However, the pH dependence can only shift the maximum of a by up to ±0.3 pH units away from the pK_a value.[19] Also it will result in an asymmetric pH profile of a, the exact shape of the profile being given by the reaction mechanism. Still, the pH profile of R_{ex} will take the same form for all the nuclei that are affected by a given protonation process.

Indeed, most of the exchange terms observed at low pH (4.2−6.5) have a pH dependence, which is in qualitative agreement with Figure 5a, as illustrated by a series of examples in Figure 5b,c. Small deviations from this trend, as illustrated in Figure S1 in the Supporting Information, most likely reflect the pH dependence of k_{ex}. Moreover, the maximum of R_{ex} for these exchange terms is close to the pK_a value of 5.1 for His92. This clearly shows that the exchange terms originate from the exchange between the protonated and deprotonated form of His92. The backbone ^{15}N of the four copper ligands are among the most affected residues, both because they are close to the side chain of His92 and because the protonation results in a rearrangement of the copper site geometry. However, the protonation/deprotonation process of His92 affects the R_2 rates of a total of 26 backbone ^{15}N nuclei, all of which have R_{ex} terms with a pH profile in accordance with this process. These residues are L7, G12, L14, F16, E17, A19, V36, H39, N40, V41, F43, H61, K62, Q63, L65, S67, F87, C89, E90, H92, R93, G94, A95, M97, V98, and G99, all of which are located within 14 Å from the copper ion.

Correction for ps−ns Dynamics. As mentioned above, small, negative R_{ex}^{app} terms arising from slow ps−ns dynamics were obtained for a number of residues, in particular outside the range where the exchange terms are pH dependent.

(39) Cho, C. H.; Urquidi, J.; Singh, S.; Robinson, G. W. *J. Phys. Chem. B* **1999**, *103*, 1991−1994.
(40) Kroenke, C. D.; Loria, J. P.; Lee, L. K.; Rance, M.; Palmer, A. G. *J. Am. Chem. Soc.* **1998**, *120*, 7905−7915.
(41) Bertini, I.; Bryant, D. A.; Ciurli, S.; Dikiy, A.; Fernández, C. O.; Luchinat, C.; Safarov, N.; Vila, A. J.; Zhao, J. *J. Biol. Chem.* **2001**, *276*, 47217−47226.
(42) Hass, M. A. S.; Led, J. J. Unpublished results.

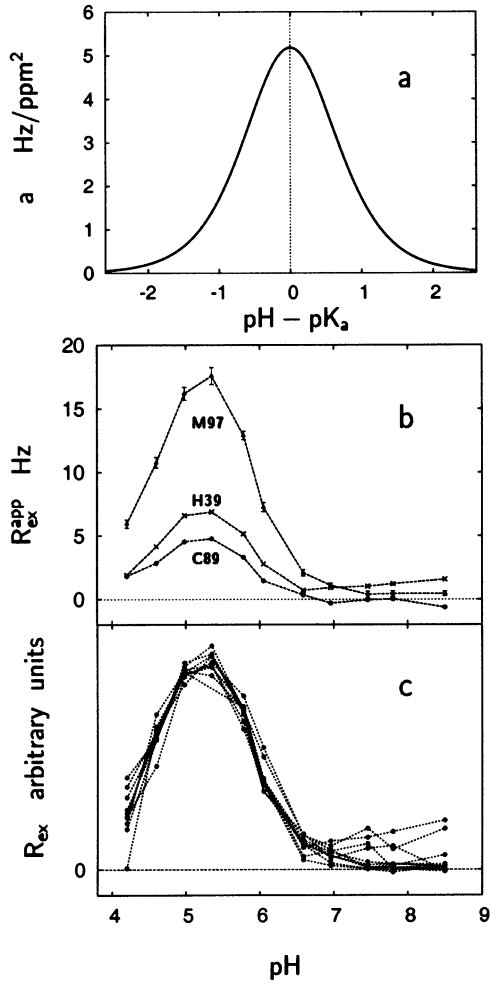

Figure 5. (a) pH dependence of the *a*-factor (eq 10) for a two-site exchange system in the fast exchange regime (eqs 8−10). The observe nucleus is ^{15}N, while $B_0 = 18.7$ T and the rate constant $k_{ex} = 10^4$ s^{-1}. The latter is assumed to be independent of the pH. (b) The approximate exchange term, R_{ex}^{app}, for the ^{15}N nuclei of three of the copper ligands plotted against pH. (c) A superposition of the pH profiles of R_{ex} for the 10 residues F16, V36, H39, N40, C89, H92, R93, A95, M97, and V98. The pH profiles are scaled by their average value.

Unfortunately, this flexibility may also affect the observed positive and pH dependent R_{ex} terms. However, an empirical correction can be made using the nonphysical, negative exchange terms observed in the region where R_{ex}^{app} is pH independent. Thus, using the pH profiles of the R_{ex}^{app} terms, correction terms, Δ_i, were estimated as the maximum negative offset observed in regions where R_{ex}^{app} is invariably negative over a range of pH values. An example of the estimation of Δ_i corrections is shown in Figure 6. The improved, corrected exchange terms, R_{ex}^{cor}, was obtained as

$$R_{ex}^{cor} = R_{ex}^{app} + \Delta_i \qquad (12)$$

assuming that Δ_i is independent of pH. This assumption is supported by the pH independence of the R_1 rates (Figure 3a).

The R_{ex}^{app} terms of 57 residues were corrected using this approach. For 17 of these residues, the Δ_i corrections were in the range from 0.2 to 0.5 Hz, and for 22 residues, they were in the range from 0.5 to 1.0 Hz. Only 4 residues have Δ_i corrections larger than 1 Hz. A list of all the estimated Δ_i terms is given in the Supporting Information.[33]

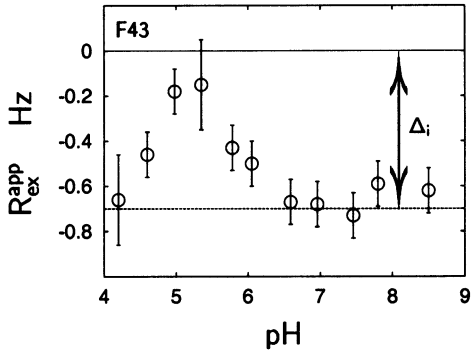

Figure 6. Approximated exchange term, R_{ex}^{app}, of Phe43 determined using eq 7. The negative values result from internal flexibility on the ps−ns time scale. The error of R_{ex}^{app} caused by this flexibility was estimated as the maximal negative offset, Δ_i. An improved, corrected exchange term, R_{ex}^{cor}, was obtained as $R_{ex}^{cor} = R_{ex}^{app} + \Delta_i$.

Qualitatively, the Δ_i terms can be interpreted as measures of enhanced ps−ns dynamics. A comparison with the backbone dynamic study of plastocyanin[26] supports this interpretation. Thus, residues with $\tau_i > 100$ ps have relatively large Δ_i corrections, as have residues with large χ^2 values in the model-free dynamics analyses.[10,11] The latter residues are likely to undergo complex ps−ns motions, which are not well accounted for by any of the applied "model-free" models. More specifically, we found that, out of the 29 residues in plastocyanin, which have either $\tau_i > 100$ ps or large χ^2 values according to the model-free study,[26] 27 residues have nonzero Δ_i corrections. Among these residues, 26 have $\Delta_i > 0.2$ Hz, while 18 have $\Delta_i > 0.5$ Hz.

Correlation between the Chemical Shift Changes and the Exchange Terms. The identification of exchange terms belonging to the same exchange process that was made in the previous section is confirmed quantitatively by the correlation between the chemical shift changes and the exchange terms. For a two-site exchange system in fast exchange, the R_{ex} is directly proportional to $\Delta\delta^2$ according to eq 9, the ratio of the two parameters being the residue-independent, exchange-rate-specific factor *a* (see eq 10). This proportionality is observed for all the 26 residues in *A.v.* PCu, which are affected by the protonation/deprotonation process of His92 according to the pH profile of their R_{ex} terms. This is shown by the plots of $\sqrt{R_{ex}^{cor}}$ versus the corresponding $|\Delta\delta|$ values in Figure 7.

Accurate values of the *a* factor were obtained by a least-squares fit to the data in Figure 7, even when only small exchange terms (≤ 1 Hz) were used, if the correction for ps−ns dynamics was made (see above). In the case of *A.v.* PCu, eq 7 provides good estimates of the exchange terms larger than 2 Hz. However, for exchange terms below 2 Hz, internal dynamics on the ps−ns time scale severely interferes with the determination of the R_{ex} terms. Yet, Figure 8 shows that the applied empirical correction of R_{ex}^{app} significantly improves the determination of R_{ex}. After the correction for ps−ns dynamics, all the 10 residues that are affected by the His92 protonation, and for which a nonzero Δ_i value was observed, are in good agreement with the value expected from the overall fit to eq 9. Thus, the errors introduced by using the simplified model, eq 7, to estimate R_2^0 are largely reduced to the size of the experimental uncertainty of R_1 and R_2. Hence, reliable estimates of R_{ex} can be obtained from the R_1 and R_2 rates alone, making

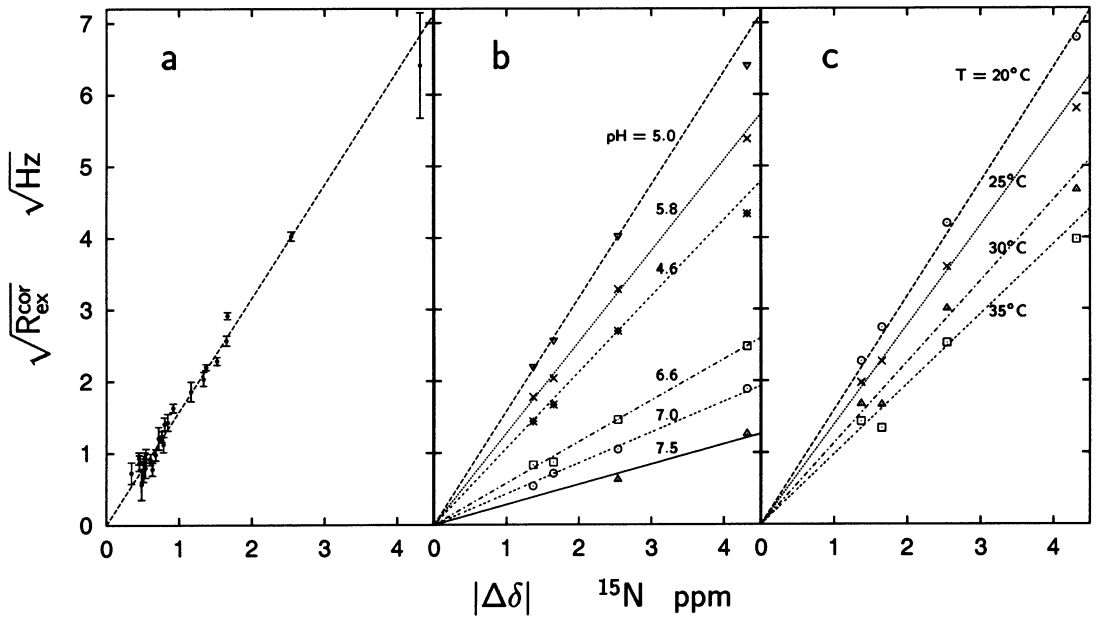

Figure 7. Square root of the exchange terms caused by the protonation of His92 in *A.v.* PCu versus the corresponding chemical shift differences $|\Delta\delta|$. The lines represent least-squares linear fits to $\sqrt{R_{ex}^{corr}} = \sqrt{a}|\Delta\delta|$ according to eq 9: (a) at pH 5.0, (b) at six different pH values, (c) at four different temperatures. For clarity, only the data for the four copper ligands are shown in parts b and c; however, the lines represent the fits to the entire data set, as specified in Table 1.

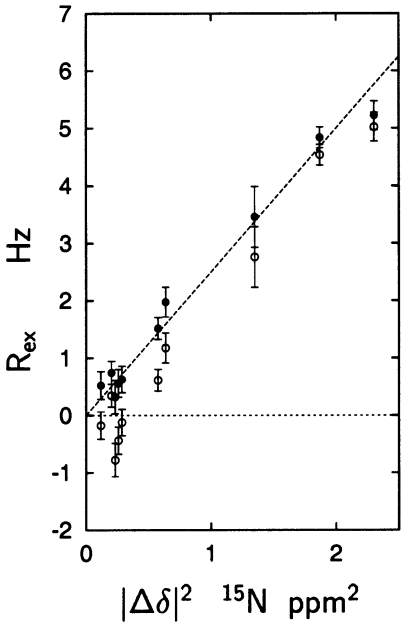

Figure 8. Approximate exchange terms, R_{ex}^{app}, (open symbols) and the corresponding corrected exchange terms, R_{ex}^{cor}, (closed symbols) versus the square of the chemical shift difference, $|\Delta\delta|$. The data are from the 10 residues that are affected by the proton exchange of His92 in *A.v.* PCu, for which Δ_i corrections were made. The R_{ex}^{app} and R_{ex}^{cor} terms were determined using eqs 7 and 12, respectively. The straight line represents the least-squares fit to the total data set in Figure 7a.

an NOE experiment unnecessary. This drastically reduces the total experimental time, which can be cut down by a factor of 3−5 when omitting the NOE experiment. Thus, one set of R_1 and R_2 experiments can be recorded in less than 24 h, which makes it feasible to obtain exchange terms, R_{ex}, at a variety experimental conditions, e.g., different pH values and temperatures, as in this study. Indeed this makes it more appealing to study the dynamics of proteins in details.

The observed proportionality between R_{ex} and $\Delta\delta^2$ is unique for a two-site exchange process. Therefore, the approach presented here allows two-site exchanges to be distinguished from multiple-site exchanges. The distinction can be made even if the involved processes have the same rate. This is in contrast to approaches based only on $R_{1\rho}$ and CPMG dispersion experiments, where a similar distinction cannot be made, unless the involved exchange rates differ by at least an order of magnitude.[14]

Also, the correlation between $\Delta\delta^2$ and R_{ex} confirms the assignment of the chemical shift changes to a specific exchange process. Since the experimental uncertainty of the R_{ex} terms is about 0.2 Hz, these terms should be at least 0.5 Hz at the maximum value of a (2.7 at pH 5.35) to be determined reliably. Consequently, $|\Delta\delta|$ must be larger than 0.4 ppm according to eq 9. A value of $|\Delta\delta| > 0.4$ ppm was determined for 30 residues. The obtained $\Delta\delta^2$ and R_{ex} values of 25 of these residues are consistent with the protonation/deprotonation process of His92. In addition, Phe43 has a pH profile in agreement with this process (see Figure 6), although its $|\Delta\delta|$ value is only 0.34 ppm. However, the backbone amide ^{15}N of the five residues Thr4, Val5, Glu30, Thr72, and Gly96 all have $|\Delta\delta|$ shifts larger than 0.4 ppm in a pH range around the pK_a value of His92; yet none of these residues have exchange terms around pH 5. Only Gly96 with a $|\Delta\delta|$ value of 0.43 ppm is close to the estimated detection limit, while Thr4, Val5, Glu30, and Thr72 have $|\Delta\delta|$ values in the range from 0.75 to 1.13 ppm, which correspond to R_{ex} terms from 1.5 to 3.4 Hz at pH 5.3, if their $\Delta\delta$ shifts were caused by the protonation of His92. Since such exchange terms are not observed, the changes in chemical shift of these residues cannot be caused by the protonation of His92. This conclusion is further supported by the magnitudes of the observed $|\Delta\delta|$ values that are surprisingly large, considering that the spatial distance of the residues from His92 is from 14 to 17 Å. However, all four residues are close to the side chain of Glu30. Therefore, it seems

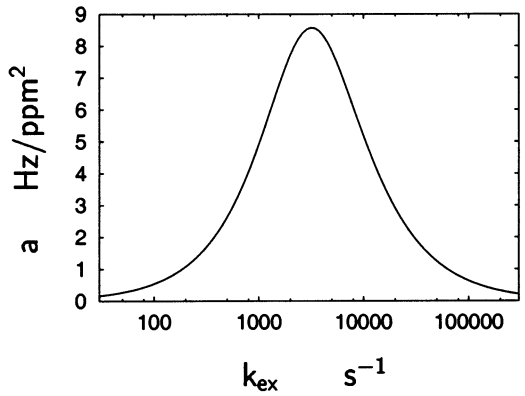

Figure 9. Simulation of the *a*-factor (eq 10) as a function of the exchange rate constant k_{ex} for the ^{15}N nuclei, illustrating that each value of *a* corresponds to two k_{ex} rate constants. The simulated curve corresponds to $B_0 = 18.7$ T, $\tau_{cp} = 1$ ms, and $p_d = p_p = 0.5$.

likely that the $|\Delta\delta|$ shifts of the four residues are caused by the protonation/deprotonation of the side chain carboxylate group of Glu30 with a pK_a of about 5.1 close to that of His92. The rate of exchange between these two states is too fast to cause any observable exchange terms, that is, $k_{ex} > 10^5$ s^{-1}.

Determination of k_{ex} for the Protonation of His92. The close correlation between the independently measured R_{ex} rates and $|\Delta\delta|$ shifts in Figures 7 and 8 allows a direct determination of the exchange rate, not only as a residual parameter determined independently for each backbone amide ^{15}N nucleus, but as a regional parameter determined simultaneously for all the ^{15}N nuclei with R_{ex} terms corresponding to the same exchange process. Thus, the k_{ex} rate constants of the protonation/deprotonation of His92 were determined over the pH range from 4.2 to 7.8, from the *a* values and the pK_a of His92, using eqs 10 and 11. Immediately, eq 10 provides two solutions for k_{ex} corresponding to a "faster" and a "slower" rate constant (see Figure 9). Both of these solutions apply only if the *fast exchange* condition is fulfilled, that is, if $k_{ex} > |\gamma B_0 \Delta\delta|$ or if $|\Delta\delta|$ is small ($\leq$3 ppm, see above).

Indeed, the *fast exchange* condition is fulfilled for all the ^{15}N nuclei affected by the protonation process of His92. This is shown by the fact that each of these nuclei in the HSQC spectra gives rise to a single well-defined signal with a continuous chemical shift titration curve in the entire pH range from 4.2 to 7.8. In contrast, in the case of *intermediate exchange* ($k_{ex} \approx |\gamma B_0 \Delta\delta|$), signals with large $|\Delta\delta|$ values would be broadened beyond detection at pH values close to the pK_a value of His92, where both states have similar populations, while, in the case of *slow exchange* ($k_{ex} < |\gamma B_0 \Delta\delta|$), two discrete signals should be observed at pH $\approx$ pK_a. Thus, the physically correct solution for k_{ex} must fulfill the fast exchange condition for all the observed ^{15}N nuclei. This holds only for the "faster" rate constant, while the "slower" one fulfills the fast exchange condition only for nuclei with $|\Delta\delta|$ values smaller than about 1.0 ppm. Hence, the true exchange rate constant is given unambiguously by the "faster" solution.

The same conclusion can be made from the temperature dependence of R_{ex}. The R_{ex} terms of the ^{15}N nuclei of *A.v.* PCu were determined at four different temperatures (20, 25, 30, and 35 °C) at pH 5.78 (Figure 7c). Qualitatively, the temperature dependence of R_{ex} defines the NMR time scale of the exchange process.[43] As shown in Figure 7c, the R_{ex} terms that originate

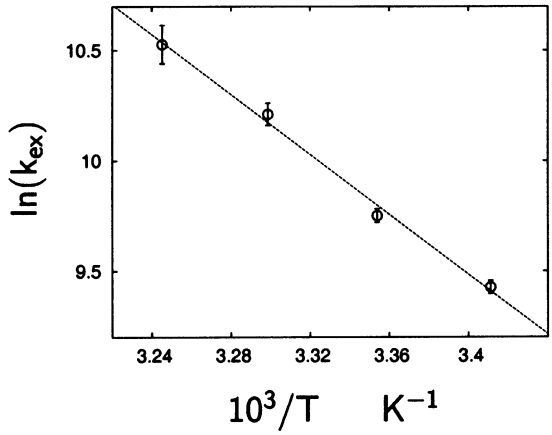

Figure 10. Arrhenius plot of the temperature dependence of the rate constant, k_{ex}, for the protonation of His92 in *A.v.* PCu at pH 5.8.

Table 1. Parameters for the Protonation/Deprotonation Process of His92 in *A.v.* PCu

pH[a]	*T*[b] °C	*n*[c]	*a*[d] Hz/ppm²	$p_d p_p$[e]	k_{ex}[d] 10^3 s^{-1}
4.20	25	23	0.85[0.04]	0.0993	27.7[1.3]
4.60	25	26	1.64[0.05]	0.1825	26.3[0.8]
4.98	25	26	2.53[0.09]	0.2453	22.8[0.8]
5.35	25	24	2.72[0.10]	0.2304	19.8[0.7]
5.78	25	26	1.94[0.06]	0.1430	17.2[0.5]
6.05	25	22	1.13[0.06]	0.0907	18.9[1.0]
6.59	25	12	0.33[0.01]	0.0304	22.0[0.7]
6.96	25	9	0.18[0.01]	0.0134	17.2[1.0]
7.46	25	5	0.08[0.01]	0.0043	12.3[1.7]
7.80	25	1	0.06[0.01]	0.0020	4.7[1.4]
8.50	25	1	0.04[0.01]	0.0004	[f]
5.78	20	26	2.54[0.08]	0.1430	12.4[0.4]
5.78	30	26	1.28[0.06]	0.1430	27.2[1.3]
5.78	35	26	0.96[0.09]	0.1430	37.3[3.5]

[a] The pH was determined from the chemical shifts in the HSQC spectrum (see Experimental Section). [b] ±0.1 °C. [c] The number of residues included in the determination of *a*. [d] Numbers in brackets are standard deviations estimated from the linear fit of *a*. [e] The product of the populations of the protonated and deprotonated states of His92, using p$K_a = 5.1$. [f] No solution could be obtained.

from the protonation of His92 decrease with increasing temperatures. Therefore, the solution of eq 10 corresponding to the "faster" k_{ex} rate constant is the actual exchange rate constant, since the solution corresponding to the "slower" constant requires the opposite temperature dependence of R_{ex}. Also the activation enthalpy, $\Delta H^{\ddagger}$, for the protonation of His92 at pH 5.8 can be estimated from the temperature dependence of k_{ex}. Thus, using the Arrhenius equation, $k_{ex} = A \exp(-\Delta H^{\ddagger}/RT)$, an activation enthalpy of 57 ± 3 kJ/mol was obtained (Figure 10), assuming that $\Delta H^{\ddagger}$, the preexponential factor, *A*, and the acid dissociation constant of the imidazole group of His92, K_a, are independent of the temperature. The latter assumption is tentative as long as $\Delta H°$ and $\Delta S°$ remain undetermined for the process. However, it seems reasonable considering the fact that the signals in the HSQC spectrum move only little in the investigated temperature range (data not shown).

The obtained exchange rates are given in Table 1. In general, the exchange rate constant is determined with a 5% accuracy. Under alkaline conditions, the population of the protonated state is low, leading to small exchange terms. Therefore, at the higher

(43) Mandel, A. M.; Akke, M.; Palmer, A. G. *Biochemistry* **1996**, *35*, 16009−16023.

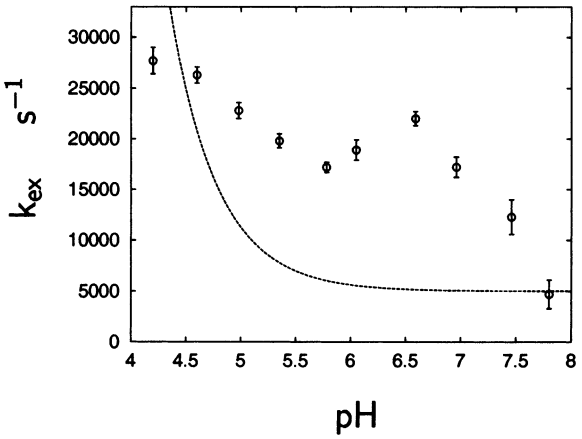

Figure 11. Exchange rate constant, k_{ex}, for the protonation/deprotonation process of His92 in *A.v.* PCu versus pH. The continuous curve corresponds to the pH dependence of k_{ex} if the proton exchange is a simple H^+ catalyzed process caused by a direct attack of H^+. In that case, $k_{ex} = k_1 + k_2[H^+]$. The curve corresponds to $k_1 = k_2K_a = 5000\ s^{-1}$ and $K_a = 10^{-5.1}$ M.

pH values exchange terms arising from the protonation process of His92 are observed only for a few residues, and at pH 7.8 only His92 has an observable exchange term. Still, it is possible to obtain the exchange rate constant with a reasonable accuracy at this pH, where only 0.2% of the molecules are protonated. However, at pH 8.5, where only 0.04% of the molecules are protonated, k_{ex} for the protonation process of His92 could not be determined.

pH Dependence of k_{ex} for the Protonation of His92. The obtained exchange rate constants for the protonation of His92 range from $28 \times 10^3\ s^{-1}$ at pH 4.2 to $5 \times 10^3\ s^{-1}$ at pH 7.8. In principle, this information provides the basis for a detailed study of the kinetics and the reaction pathway of the exchange process. Previously the protonation/deprotonation of imidazole groups has been modeled as a specific-acid catalysis, a specific-base catalysis, or a combination of both where H^+ or OH^- ions catalyze the protonation or deprotonation, respectively.[19] However, none of these models agree with the pH dependence of the protonation rate of His92 shown in Figure 11. Although the exchange rate constant first decreases from pH 4.2 to 5.8 in qualitative agreement with an H^+ catalysis, it subsequently increases again until about pH 6.6 and finally decreases rapidly at higher pH. This unusual dependence strongly suggests a more complex pathway for the protonation process of His92. Considering the care that was exercised in preparing and stabilizing the samples (see Experimental Section), we can exclude that the observed pH dependence of k_{ex} results from a general-acid−base catalysis by impurities in the samples or from a slight oxidation of the plastocyanin in some of the samples.

Instead, the protonation of His92 may take place through different pathways and by different mechanisms, depending on the pH. These pathways and mechanisms may involve catalyses by acidic or basic side chains, breaking of the Cu^+−N bond, a rotation of the His92 imidazole group, or other structural and chemical changes. Also cooperativity between proton binding sites may systematically distort the derived exchange rates. To further clarify the mechanism of the protonation process of His92 in *A.v.* PCu, a detailed investigation of these possibilities is in progress.

Protonation of His61. Exchange terms that are strongly pH dependent around pH 7 were observed for the 18 residues H39, V41, V42, L59, S60, H61, K62, Q63, L64, M66, S67, G69, Q70, T72, S73, T74, T75, and D79. These residues are all grouped around the imidazole of His61, and a change in chemical shift was observed for all 18 residues at pH values around 7.1 (see Figure 2b and d).

However, in contrast to the protonation/deprotonation of His92, there is no unique linear correlation between the R_{ex} terms and the chemical shift differences between protonated and deprotonated forms (see Figure 12a). Immediately, this shows that the protonation/deprotonation of His61 is at least a three-site exchange process. Furthermore, the R_{ex} terms for different residues depend differently on pH, as shown in Figure 12b. The R_{ex} rates for all 18 residues increase up until pH 7, but above this pH, their pH profiles are different as illustrated in Figure 12b. Some of the residues have decreasing R_{ex} rates above pH 7, most pronounced His61, while other residues have R_{ex} rates that continue to increase, one example being Lys62. These differences in the pH profiles of the R_{ex} rates above pH 7.0 clearly indicate the presence of an additional exchange process which, furthermore, involves only the deprotonated form of His61. The simplest model for this exchange system is a three-site exchange model consisting of two processes,

$$[A \rightleftarrows B] + H^+ \rightleftarrows CH^+ \qquad (13)$$

One of these processes is the exchange between the protonated state and the average deprotonated state. The other process is an exchange between two deprotonated states, A and B, as shown in eq 13. The observed exchange term is the sum of the exchange terms for the two processes. The two contributions can in principle be separated by their pH dependence. However, the analysis is complicated by the pH dependence of the exchange rates, which remains unknown.

Still, for some of the nuclei with pH dependent exchange terms around pH 7, the R_{ex} terms are affected predominately by the protonation process, while they are nearly unaffected by the exchange between the deprotonated allo-states. In these cases, the exchange process can be approximated by the two-site model, and k_{ex} for the protonation process can be estimated. The nuclei belonging to this group all have exchange terms that decrease strongly at pH above the pK_a value of His61, thus resulting in pH profiles qualitatively similar to Figure 5. This trend is most pronounced for the residues V41, V42, H61, and T72, as illustrated in Figure 12d. Consequently, the exchange terms of these four residues are in agreement with the two-site model. Again, this is supported by the linear correlation between their R_{ex} and $\Delta\delta^2$ values, as shown in Figure 12c. We note that the two-site approximation may not apply at pH values above the pK_a value of His61, where the deprotonated states are more abundant than the protonated state, making the R_{ex} terms affected also by the exchange process between the different deprotonated states. Therefore, only the R_{ex} terms in the range from pH 6 to 7 were used in the two-site exchange model analysis. Moreover it can be assumed that the protonation process of His61 is in *fast exchange*, as indicated by the continuous titration curves obtained for all the affected residues. As for His92, the latter assumption identifies the "faster" solution of eq 10 as the actual exchange rate constant.

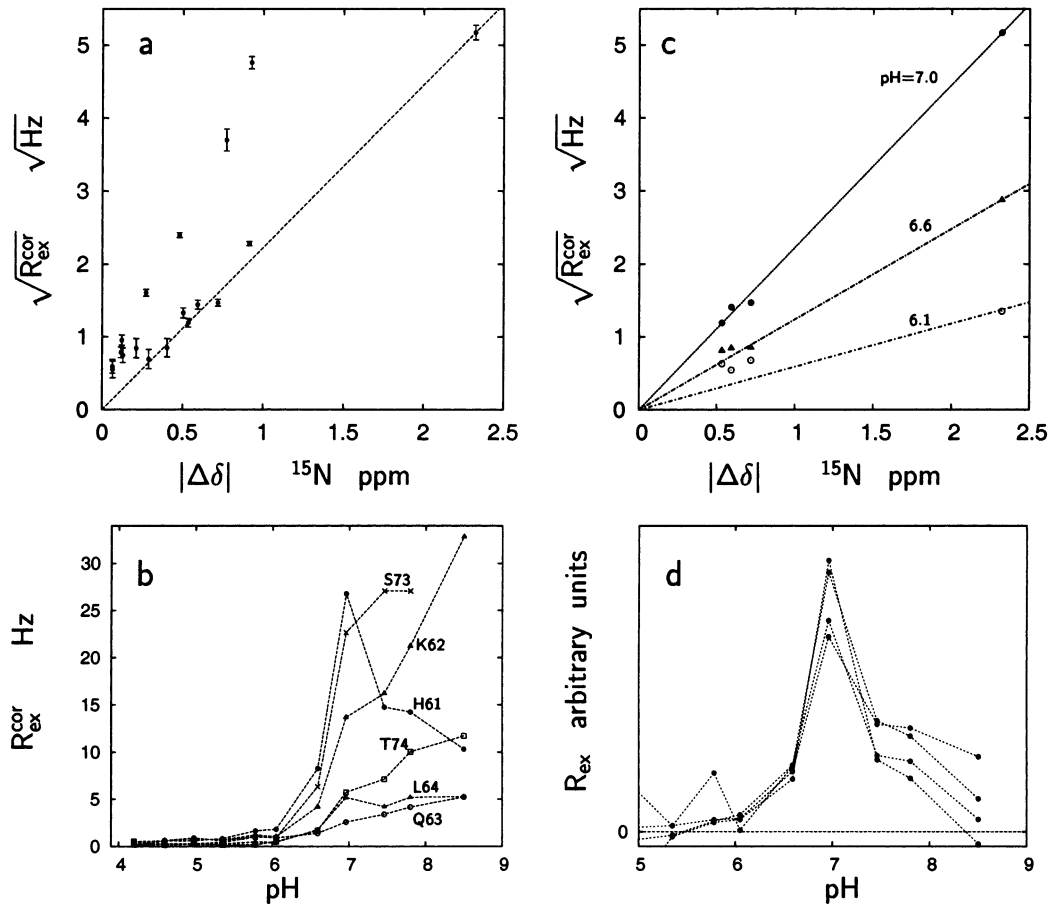

Figure 12. (a) Square root of the 18 backbone ^{15}N exchange terms, R_{ex}^{cor}, related to the protonation of His61 in *A.v.* PCu versus the corresponding chemical shift difference, $|\Delta\delta|$, at pH 7.0. (b) The pH dependence of R_{ex}^{cor} for six residues, illustrating the difference in pH dependence observed for the residues affected by the protonation of His61. (c) As in part a but for the four residues V41, V42, H61 and T72 that are closest to a two-site exchange model according to the correlation between R_{ex} and $|\Delta\delta|$.[2] The data in part c correspond to the three different pH values 6.1, 6.6, and 7.0. The lines represent least squares linear fits to $\sqrt{R_{ex}} = \sqrt{a}|\Delta\delta|$, eq 9. (d) The pH profiles of the four residues in part c scaled by their average value.

Table 2. Parameters for the Protonation/Deprotonation Process of His61 in *A.v.* PCu

pH	a [a] Hz/ppm^2	$p_d p_p$ [b]	k_{ex} [a] 10^3 s^{-1}
6.05	0.35[0.05]	0.0751	54[8]
6.59	1.54[0.03]	0.1803	28[1]
6.96	4.96[0.05]	0.2436	10.3[0.1]

[a] Numbers in brackets are standard deviations estimated from the linear fit of a including data from four residues obtained a 25 °C. [b] The product of the total population of deprotonated states and the population of the protonated state using pK_a = 7.1.

As shown in Table 2, the obtained rate constant decreases rapidly with increasing pH in the range pH 6−7. This suggests that an acid catalysis is the major pathway for the protonation of His61. The exchange between the two deprotonated allostates could involve a reorientation of the side chain of His61 and a tautomerization and/or a rearrangement of the hydrogen bonding of the aromatic N−H of the imidazole group. However, a more detailed analysis of the mechanism based on the three-site exchange model requires reliable exchange rate constants also above pH 7 and a better characterization of the exchange process involving only the deprotonated state. Also, additional experimental information is needed for a determination of all the parameters included in the three-site model. To that end, $R_{1\rho}$ measurements may prove useful.

Other Exchange Processes in Plastocyanin. The R_{ex} exchange terms observed for *A.v.* PCu originate primarily from the protonations and deprotonations of His92 and His61. However, for a series of residues, small exchange terms are observed that cannot be accounted for by the histidine protonations. Thus, the pH profiles of these residues do not correspond to the histidine protonations, or the $R_{ex}/\Delta\delta^2$ ratios of the residues do not agree with the *a*-factors in Tables 1 and the correlations in Figure 7. Thus, residues with pH profiles that do not agree with the histidine protonations are A45, A46, A50, A56, K57, A82, and T86, which all have pH *independent* exchange terms ranging from 0.3 to 1.0 Hz. These residues are all located in the "south east corner" of PCu, which includes the α helix. The pH independent exchange terms indicate that the "south east corner" has an enhanced flexibility on the μs−ms time scale, as suggested by previous studies.[26,41] Also, a number of exchange terms arise at very low pH. These exchange terms are most likely associated with the protonation of aspartate and glutamate residues and may be the first signs of a destabilization of the protein structure, which ultimately leads to denaturation at low pH.

Finally Val36, which is close to the imidazole group of His92, appears to have an additional contribution to the exchange term of about 1.5 Hz. Primarily, the R_{ex} terms of Val36 are dominated by the protonation process of His92. However, if R_{ex} is

recalculated from the measured chemical shift difference using the *a*-factors of the His92 protonation, R_{ex} terms that are significantly smaller than the observed value are obtained below pH 6.5. Above this pH value, signal overlap with Tyr88 results in unreliable R_{ex} estimations. Tentatively, this suggests an additional exchange process in the proximity of Val36.

Relaxation Effects from Solvent Exchange. A series of residues have R_{ex} terms that are caused by exchange of the amide protons with the solvent. This is the case for the 10 residues T2, D10, K11, T22, A45, A53, D54, L55, G94, and G96, all of which have amide protons that exchange relatively fast with the solvent water[35] while still giving rise to separate amide proton signals. Moreover, as a result of the amide proton exchange, the intensities of these signals in the HSQC spectra decrease drastically at high pH. Thus, the signals of residue D10, K11, A53, D54, and G94 were unobservable in the HSQC spectrum at the higher pH values applied here.

All the 10 residues have small R_{ex} terms that increase with increasing pH, reaching a maximum value of 1−3 Hz at the higher pH values. We suggest that these exchange terms reflect a scalar R_2 relaxation of the second kind[44] caused by the large scalar coupling interaction ($^1J_{^{15}N^1H} \approx 92$ Hz) between the proton and ^{15}N nucleus of the amide group and modulated by the exchange of the amide protons with the solvent. Although, this effect is suppressed by the CPMG pulse sequence, it still contributes significantly to the ^{15}N R_2 rates if the exchange rate is close to $2\pi J$. In cases where the exchange rate is faster than $2\pi J$, these signals disappear in the HSQC spectrum, as observed here, since the exchange modulation effectively decouples the scalar interaction, thereby preventing the magnetization to be transferred by the INEPT sequences in the HSQC experiment.

Concluding Remarks

The study here demonstrates the feasibility of obtaining detailed, quantitative information about conformational exchange processes in proteins on the μs−ms time scale, by a combined analysis of the NMR relaxation caused by the exchange process and the difference in chemical shift between the exchanging species. It also illustrates the usefulness of acquiring relaxation data at various sample conditions. Thus, a large number of exchange terms have been assigned, unambiguously, to two specific exchange processes, namely the protonation/deprotonation of His92 and His61, respectively. Also, the approach has enabled us to decide that the protonation/deprotonation of His92 follows a two-site exchange scheme, while the corresponding process for His61 is coupled to an exchange between different conformations of the deprotonated state, resulting in, at least, a three-site exchange process. Moreover, in the case of the two-site exchange process, the exchange rate is determined as a *regional* parameter from the exchange terms of a large number of nuclei.

The success of the approach suggests that it will prove useful in the studies of other systems involving conformational exchange on the μs−ms time scale. Such systems may include enzymes with pH-titratable side chains in the active site, especially histidines and cysteins, where the approach could be used to investigate the active site dynamics in detail. The approach can also be valuable in the studies of systems where a ligand other than a proton binds specifically to the protein, as for instance the binding of a diamagnetic metal ion.

Interactions of proteins with small organic molecules, peptides, other proteins, or polynucleotides can also be studied using the approach presented here. In general, it is required that the binding is specific, that a number of ^{15}N chemical shifts are significantly affected, and that the binding and unbinding occur on the μs−ms time scale. The approach will allow investigations of the kinetics of both *inter*molecular and *intra*molecular processes and the relation between such processes. Thus, allosteric activation, cooperativity, and enzyme catalysis may be studied at the atomic level. In this context, it will be important to resolve the three-site or four-site exchange schemes that are expected for these processes, namely the binding and unbinding of a ligand coupled to a conformational exchange of the protein structure. Here, additional information is required in order to determine all the parameters describing the three-site exchange system. This information could be obtained from $R_{1\rho}$ or CPMG relaxation dispersion experiments or from line shape analyses of the ligand signals.

Experimental Section

Construction of an *E. coli* Strain which Overexpresses *A.v.* PCu. Recombinant *A.v.* PCu was heterologously produced in *E. coli* BL21G-(DE3) (Stratagene) from the pET3a plasmid vector (Novagen)[45] containing the structural gene flanked by a *Nde*I and a *Bam*HI restriction enzyme cleavage sites. The following sense primer 5′-CAT ATG GAA ACA TAC ACA GTA AAA CTA-3′ and antisense primer 5′-GGA TCC CTA GCC GGC GAC AGT GAT-3′ based on the GenBank L19417 sequence[46] was used. The gene was amplified by thermal cycling directly from *A. variabilis* cells (strain ATCC 29413) using *Pyrococcus furiosus* DNA (Turbo) polymerase (Stratagene), while following the protocol provided by the manufacturer. The amplified DNA fragment was cloned into the pPCR−Script Amp SK vector (Stratagene). The DNA sequence was confirmed using a BigDye terminator chemistry protocol (Applied Biosystems) and analyzed on an ABI310 (Applied Biosystems) DNA sequencer. The *A.v.* PCu encoding *Nde*I/*Bam*HI DNA fragment was ligated with a similarly digested pET3a plasmid. The resulting plasmid was transformed into *E. coli* BL21G(DE3) cells. Recombinant DNA techniques were used according to standard protocols.

Overexpression and Purification of ^{15}N-Labeled *A.v.* PCu. The *A.v.* PCu producing *E. coli* strain was grown at 30 °C in ^{15}N-enriched rich growth medium Eco-*E. coli*-OD N (Silantes) containing 100 μg/mL ampicillin. The cell culture was grown aerobically to an OD_{600} of 0.6, before the recombinant protein production was induced by addition of IPTG to a concentration of 0.1 mM. After 4 h of incubation, the cells were harvested by centrifugation, and the pellet was stored at −80 °C. The recombinant protein was released from the cells during three successive freeze (−80 °C)/thaw (4 °C) cycles.[47] Subsequently, the pellet was resuspended in 0.5 mM $MgCl_2$ and incubated on ice for 25 min with periodic gentle agitation. The supernatant was collected by centrifugation, and $CuSO_4$ was added to a final concentration of 0.5 mM followed by incubation on ice for 30 min. The protein extract was diluted with water to a conductivity of 300 μS/cm, and the blue plastocyanin was captured on an SP Sepharose Fast Flow column (Amersham Biosciences) equilibrated with 5 mM MES/NaOH pH 6.5. The column was washed with 5 mM MES/NaOH pH 6.5, and the plastocyanin was eluted with 5 mM MES/NaOH pH 6.5, 60 mM NaCl.

(44) Abragam, A. *Principles of Nuclear Magnetism*; Clarendon Press: Oxford, 1961; pp 309−312.
(45) Studier, F. W.; Rosenberg, A. H.; Dunn, J. J.; Dubendorff, J. W. *Methods Enzymol.* **1990**, *185*, 60−89.
(46) Ghassemian, M.; Wong, B.; Ferreira, F.; Markley, J. L.; Straus, N. A. *Microbiology* **1994**, *140*, 1151−1159.
(47) Ybe, J. A.; Hecht, M. H. *Protein Expression Purif.* **1994**, *4*, 317−323.

Subsequently, the plastocyanin was exchanged into 5 mM MES/NaOH pH 6.5 by ultrafiltration, using a stirred Amicon cell fitted with a YM3 membrane. The *A.v.* PCu was finally purified to apparent homogeneity on an ÄKTA purifier (Amersham Biosciences) HPLC system equipped with a Source 30 S column (Amersham Biosciences) using a linear gradient of 0−75 mM NaCl in 5 mM MES/NaOH pH 6.5. Approximately 7 mg per l culture of pure plastocyanin with a peak ratio A_{278}/A_{597} of 1.18 was obtained. This peak ratio value is identical to the value obtained for native *A. variabilis* plastocyanin.[48]

NMR Samples. Freshly purified *A.v.* PCu solutions were exchanged into 10%/90% D_2O/H_2O, 100 mM NaCl, and concentrated by ultrafiltration using a stirred Amicon cell fitted with a YM3 membrane. Sodium ascorbate (0.1 mM) was added to all samples to keep the sample fully reduced.

A 2 mM sample of ^{15}N labeled *A.v.* PCu was used for the chemical shift titration experiment. The pH was adjusted by adding small amounts of NaOH or HCl. The pH in the sample measured by a pH meter before and after the recording of each spectrum varied less than 0.1 units. The effective pH in the sample during acquisition was estimated as the average of the two measured pH values. To ensure that the sample was fully reduced, small additional amounts of sodium ascorbate were added several times during the series of titration experiments and the sample was sealed under N_2.

The relaxation measurements were performed on five 1.0 mM ^{15}N labeled *A.v.* PCu samples prepared from the same stock solution but with different pH. The ^{15}N relaxation rates in PCu are highly sensitive to the sample conditions, and the success of the study relies heavily on the stability of the samples and the quality of the obtained data. Thus, even small amounts (less than 1%) of oxidized (paramagnetic) PCu can significantly affect the relaxation rates, while buffer molecules as well as products from peptide hydrolysis of denatured protein may catalyze protonation processes. Therefore, in addition to adding small additional amounts of ascorbate (see above) and omitting buffers, the samples used for the relaxation measurements were sealed off under N_2 immediately after preparation and were at no time thereafter exposed to oxygen. Furthermore, the redox state of the PCu samples was monitored using the ^{15}N R_1 rates of Asn40 and His92, which are the two residues with the largest paramagnetic contributions to their backbone ^{15}N R_1 rates in the oxidized form of the protein.[36] Thus, a concentration of oxidized PCu as low as 1 μM would be revealed by an enhanced R_1 rate of these residues. After acquisition, the five samples were opened once (one sample twice) under N_2, and the pH was changed by adding small amounts of HCl or NaOH. Following this procedure, a total of 11 samples with different pH values in the range from pH 4.20 to pH 8.50 were prepared for the relaxation studies.

NMR Spectroscopy. All NMR experiments were carried out on a Varian Inova 800 spectrometer operating at a magnetic field strength of 18.7 T, corresponding to an ^{1}H frequency of 799.76 MHz and an ^{15}N frequency of 81.05 MHz. The pH dependence of the ^{15}N chemical shifts of the backbone amide groups was determined from a series of ^{15}N-HSQC spectra recorded at 17 different pH values, using a standard gradient enhanced pulse sequence.[49] The sweep widths in the ^{1}H and the ^{15}N dimension were 13 000 and 3200 Hz, respectively. The numbers of complex data points acquired in the two dimension were 2130 and 180, respectively.

Standard HSQC based R_1 and R_2 experiments, as described by Farrow et al.,[9] were recorded. Eight scans were acquired for each FID, using sweep widthss of 13 000 and 3400 Hz in the ^{1}H and ^{15}N dimension, respectively. Again the numbers of complex data points were 2130 and 180, respectively. Each R_1 experiment consisted of eight spectra with different relaxation delays ranging from 0.01 to 1.9 s, while the R_2 experiments consisted of 10 to 12 spectra with relaxation delays ranging from 0.0 to 176 ms. In the ^{15}N R_2 experiments, a CPMG pulse was applied to the protons and the ^{15}N nuclei.[9] The interpulse delays, τ_{cp}, in the CPMG pulse were 8 ms for ^{1}H and 1 ms for ^{15}N. The total acquisition time for one set of experiments including one HSQC spectrum, one R_2 experiment, and one R_1 experiment was about 23 h.

All the relaxation experiments were carried out over a continuous period of 3 weeks to minimize effects from protein degradation, and the relaxation series were performed in random order. Moreover, the individual relaxation experiments were recorded using a recurrent procedure[36] that ensures that all the 2D slices of a given relaxation experiment were effectively recorded over the same period of time. Also, the relaxation delays were chosen in random order, to further minimize errors from temperature instability during an experiment.

Data Analysis. The ^{1}H and ^{15}N spectra of native *A.v.* PCu were assigned previously.[26] The recombinant PCu used here differs from the native protein by having a methionine residue added to the N-terminus. However, no significant differences between the HSQC spectra of the recombinant and the native *A.v.* PCu were observed. Also, the individual signals in the spectra could easily be followed over the investigated pH range (4.2−8.5). The effective pH of the sample during the R_2 experiments was determined from the chemical shifts in an HSQC spectrum recorded immediately prior to the R_2 experiment, using the chemical shift pH dependences determined in the chemical shift titration experiments (see above). Several signals were used, and the final pH was calculated as the average value. Based on the deviations of the pH values obtained from different signals, the error was estimated to be less than 0.05 pH units. The relaxation rates were obtained from a two-parameter least-squares fit of a single-exponential decay to the time dependencies of the signals intensities, measured as the peak heights. The isotropic rotational correlation time and the global R_2/R_1 ratio were determined from the 15% trimmed average, as described previously.[26] Residues with significant exchange terms were excluded from the average.

Acknowledgment. We thank Malene R. Jensen, D. Flemming Hansen, Søren M. Kristensen, Henrik Gesmar, and Jens Ulstrup for helpful discussions and Lise-Lotte Jespersen, Else Philipp, Jens Duus, and Bent O. Petersen for technical assistance. The 800 MHz spectra were acquired at The Danish Instrument Center for NMR Spectroscopy of Biological Macromolecules. M.A.S.H. thanks Novo Nordisk A/S and Novozymes A/S for a scholarship. This work was financially supported by the Danish Natural Science Research Council (J. No. 9400351, 51-00211, and 21-01-0545) and Novo Nordisk Fonden.

Supporting Information Available: Tables of the backbone ^{15}N chemical shift titration parameters of *A.v.* PCu, the experimental ^{15}N R_1 and R_2 relaxation rates, the derived R_{ex} terms at pH 4.6 and 8.5, and the estimated correction terms, Δ_i. This material is available free of charge via the Internet at http://pubs.acs.org.

JA030366M

(48) Christensen, H. E. M.; Conrad, L. S.; Ulstrup, J. *Photosynth. Res.* **1990**, *25*, 73−76.
(49) Zhang, O.; Kay, L. E.; Olivier, J. P.; Forman-Kay, J. D. *J. Biomol. NMR* **1994**, *4*, 845−858.